forests

MDPI

Article

Using a Bottom-Up Approach to Scale Leaf Photosynthetic Traits of Oil Palm, Rubber, and Two Coexisting Tropical Woody Species

Ashehad A. Ali [1,*], Braninditiyo Nugroho [1], Fernando E. Moyano [1], Fabian Brambach [2], Michael W. Jenkins [3], Robert Pangle [3], Christian Stiegler [1], Emanuel Blei [1], Andi Nur Cahyo [4], Alexander Olchev [5], Bambang Irawan [6], Rahmi Ariani [1], Tania June [7], Suria Tarigan [8], Marife D. Corre [9], Edzo Veldkamp [9,10] and Alexander Knohl [1,10]

1 Department of Bioclimatology, University of Göttingen, Büsgenweg 2, 37077 Göttingen, Germany; bramngrh@gmail.com (B.N.); fmoyano@uni-goettingen.de (F.E.M.); christian.stiegler@biologie.uni-goettingen.de (C.S.); eblei@gwdg.de (E.B.); rahmi.ariani@gmail.com (R.A.); aknohl@uni-goettingen.de (A.K.)
2 Biodiversity, Macroecology & Biogeography, University of Göttingen, Büsgenweg 1, 37077 Göttingen, Germany; fbrambach@uni-goettingen.de
3 Rubisco Research and Consulting, 7424 S University Blvd, Boulder, CO 80122, USA; mike@rubiscoconsulting.com (M.W.J.); rob@rubiscoconsulting.com (R.P.)
4 Indonesian Rubber Research Institute, Balai Penelitian Sembawa, Palembang 30953, Indonesia; nurcahyo.andi@yahoo.co.uk
5 Department of Meteorology and Climatology, Lomonosov Moscow State University, Ulitsa Kolmogorova, 119991 Moscow, Russia; aoltche@gmail.com
6 Faculty of Forestry, University of Jambi, Kabupaten Muaro Jambi, Jambi 36122, Indonesia; irawanbam@yahoo.com
7 Department of Geophysics and Meteorology, Bogor Agricultural University, Kampus IPB Dramaga Bogor, Bogor 16680, Indonesia; tania.june@yahoo.com
8 Department of Soil and Natural Resources Management, Bogor Agricultural University, Kampus IPB Dramaga Bogor, Bogor 16680, Indonesia; suriatarigan2014@gmail.com
9 Soil Science of Tropical and Subtropical Ecosystems, University of Göttingen, Büsgenweg 1, 37077 Göttingen, Germany; mcorre@gwdg.de (M.D.C.); eveldka@gwdg.de (E.V.)
10 Centre of Biodiversity and Sustainable Land Use, University of Göttingen, Büsgenweg 1, 37077 Göttingen, Germany
* Correspondence: ashehad.ali@uni-goettingen.de or ali.ashehad@gmail.com; Tel.: +49-5513-933685

check for updates

Citation: Ali, A.A.; Nugroho, B.; Moyano, F.E.; Brambach, F.; Jenkins, M.W.; Pangle, R.; Stiegler, C.; Blei, E.; Cahyo, A.N.; Olchev, A.; et al. Using a Bottom-Up Approach to Scale Leaf Photosynthetic Traits of Oil Palm, Rubber, and Two Coexisting Tropical Woody Species. *Forests* **2021**, *12*, 359. https://doi.org/10.3390/f12030359

Received: 17 February 2021
Accepted: 16 March 2021
Published: 18 March 2021

Abstract: Rainforest conversion to woody croplands impacts the carbon cycle via ecophysiological processes such as photosynthesis and autotrophic respiration. Changes in the carbon cycle associated with land-use change can be estimated through Land Surface Models (LSMs). The accuracy of carbon flux estimation in carbon fluxes associated with land-use change has been attributed to uncertainties in the model parameters affecting photosynthetic activity, which is a function of both carboxylation capacity (V_{cmax}) and electron transport capacity ($J_{\max}$). In order to reduce such uncertainties for common tropical woody crops and trees, in this study we measured V_{cmax25} (V_{cmax} standardized to 25 °C), $J_{\max 25}$ ($J_{\max}$ standardized to 25 °C) and light-saturated photosynthetic capacity ($A_{\max}$) of *Elaeis guineensis* Jacq. (oil palm), *Hevea brasiliensis* (rubber tree), and two native tree species, *Eusideroxylon zwageri* and *Alstonia scholaris*, in a converted landscape in Jambi province (Sumatra, Indonesia) at smallholder plantations. We considered three plantations; a monoculture rubber, a monoculture oil palm, and an agroforestry system (jungle rubber plantation), where rubber trees coexist with some native trees. We performed measurements on leaves at the lower part of the canopy, and used a scaling method based on exponential function to scale up photosynthetic capacity related traits to the top of the canopy. At the lower part of the canopy, we found (i) high V_{cmax25} values for *H. brasiliensis* from monoculture rubber plantation and jungle rubber plantation that was linked to a high area-based leaf nitrogen content, and (ii) low value of $A_{\max}$ for *E. guineensis* from oil palm plantation that was due to a low value of V_{cmax25} and a high value of dark respiration. At the top of the canopy, $A_{\max}$ varied much more than V_{cmax25} among different land-use types. We found that photosynthetic capacity declined fastest from the top to the lower part of the canopy in oil palm

plantations. We demonstrate that photosynthetic capacity related traits measured at the lower part of the canopy can be successfully scaled up to the top of the canopy. We thus provide helpful new data that can be used to constrain LSMs that simulate land-use change related to rubber and oil palm expansion.

Keywords: photosynthesis; plant traits; land-use types; land surface models

1. Introduction

Tropical forest conversions to different land use significantly impact water and carbon cycle dynamics by modifying carbon sequestration and carbon emission rates [1,2]. In Southeast Asia, Indonesia has one of the highest annual losses of rainforests worldwide [3], where forests have been deforested and converted to woody croplands, namely oil palm and rubber plantations [4]. One of the hotspots of land-use change in Indonesia has been Jambi's province in Sumatra Island, where the area of rubber plantations increased by 19%, and that of oil palm plantations by 85%, from 2000 to 2010 [5]. Land-use change (LUC) from native forest vegetation to rubber and oil palm plantations has increased the income of farmers of Jambi [4,6,7] while at the same time leading to significant ecological costs: decreases in above-ground and below-ground carbon stocks [8–10], reduction in soil nitrogen availability [11] and increases in soil N_2O emissions following N fertilization [12]. Partly because of a lack of field data, it is still unclear to what extent these changes will impact water and carbon transfer between land surface and atmosphere. In consequence, and despite their importance for biogeochemical cycles, the impacts of LUC in the tropics are not well represented in Land Surface Models (LSMs).

In LSMs, the exchange of gases between plants and the atmosphere is represented at the leaf and canopy levels. One common method used to calculate fluxes of carbon and water vapor is the coupling of a mechanistic C_3 model of assimilation FvCB [13] to a stomatal conductance model (gs; Ball, Woodrow & Berry 1987 [14]). In the FvCB model, net leaf photosynthesis (A_n) of C_3 plants is simulated with the assumption that A_n is equal to the lowest rate of three limiting biochemical processes: (1) the ribulose 1.5-bisphosphate (RuBP) saturation rate under low intercellular CO_2 concentrations (C_i), where the rate of A_n is predicted by the properties of the Rubisco enzyme (V_{cmax}); (2) the rate of regeneration of RuBP at high C_i, driven by light harvesting and electron transport (J_{max}); or (3) triose phosphate use limitation (TPU) [15]. Recent studies have shown that TPU rarely limits net photosynthesis [16,17]. To our knowledge, many LSMs do not consider TPU limitation or represent it non-mechanistically [18,19], as the evidence for the occurrence of TPU limitation in mature plants from natural ecosystems is scarce (Ellsworth et al. 2015 [20]).

Thus, photosynthetic capacity in LSMs is mainly represented by V_{cmax} and J_{max}, whose values are estimated from A_n/C_i curves. These parameters are often coupled, allowing J_{max} to be estimated from V_{cmax} [21,22]. V_{cmax} and J_{max} values in LSMs are frequently treated as fixed per plant functional type or linearly related to leaf nitrogen [23,24]. While V_{cmax} and J_{max} have been shown to have a substantial impact on global projections of the carbon cycle [25,26], the natural variability of these parameters is still not known for many plants or ecosystem types.

Since photosynthetic capacity is commonly expressed as the light-saturated photosynthetic rate (A_{max}) [27–30], we measured light response curves in addition to CO_2 response curves. Although we are aware that recently there has been standardization in the format of leaf gas exchange parameters [31], in this study we refer to A_{max} as the typical maximum photosynthetic rate under optimal conditions in the field [30,32–34], so that we can compare our estimates with the literature. We estimated A_{max}, V_{cmax25} and J_{max25} (J_{max} standardized to 25 °C) of rubber trees (*H. brasiliensis*) and oil palms (*E. guineensis*) in smallholder farmers monoculture plantations, as well as from a jungle rubber plantation [35], where rubber trees coexist with native trees [35,36]. In our study region, the tree species *A. scholaris* and *E.*

zwageri are commonly found to coexist with rubber trees [9,29,37]. *A. scholaris* is considered to be a light-demanding species, and is principally grown for timber production [29], while *E. zwageri* is a mid-canopy species [37] and grows relatively slowly [38,39].

In this study, our aim is to determine the photosynthetic capacity and foliar traits of oil palm, rubber and two coexisting woody species growing in tropics. We limited our field measurements at the lower part of the canopy due to logistic constraints. Since estimates of V_{cmax25} and J_{max25} at the lower part of the canopy are not directly useful to the LSMs, we used a scaling method based on exponential function to scale up photosynthetic capacity-related traits to the top of the canopy [25,40,41]. The scaling method assumes that photosynthetic capacity at the canopy top is scaled with depth, such that photosynthetic capacity at the canopy top decreases exponentially with cumulative leaf area index [25]. The main objectives of our study were: (i) to estimate key physiological parameters (V_{cmax25}, J_{max25}, A_{max}) and leaf traits (LMA, leaf N), in two tropical tree crops (rubber and oil palm) and two native tree species at the lower part of the canopy; and (ii) to scale up photosynthetic capacity-related traits measured at the lower part of the canopy to the top of the canopy using a 'bottom-up' approach.

2. Methods

2.1. Experimental Sites

We conducted our measurements in Jambi Province of the island of Sumatera, Indonesia. The region's climate is tropical maritime, and the rainy season goes from October through April, with the rest of the year being relatively dry [42–44]. The average monthly rainfall in the drier season (161 mm month^{-1}) is 38% lower than in the rainy season (261 mm month^{-1}). The mean annual temperature and mean annual precipitation measured at Jambi airport are 26.7 ± 0.2 °C and 2235 ± 381 mm, respectively [42,45]. Measurements were conducted in three land-use types on loam Acrisol soils: a monoculture oil palm plantation (S 01°54′34.6″ E 103°15′58.3″), a monoculture rubber plantation (S 01°54′39.5″ E 103°16′00.1″), and a jungle rubber plantation, where rubber trees are planted within secondary forests (S 01°55′40.0″ E 103°15′33.8″) [9]. All study sites were owned by local smallholders. The oil palm plantation was 16 years old at sampling, with an average height of 12 meters [9]. The oil palm plantation received fertilization rates of 68-30-99 kg N, P, K ha^{-1} year^{-1} [46].

The rubber trees in the monoculture rubber plantation and jungle rubber were of similar age (about 14 years old), with an average height of 13 meters, and the monoculture rubber plantation, jungle rubber plantation and oil palm stem density were about 440 ha^{-1} and 525 ha^{-1} and 140 ha^{-1}, respectively [9]. Rubber cultivars differ in clone types [47]. In Sumatra, the most widely planted clone is PB 260 [48], which is characterized by a high production potential and strength against wind disturbances [49]. It is also one of the latex-producing clones recommended for their high yield characteristic [50]. In contrast, there is no single oil palm cultivar used in Jambi. Based on local farmers' communication, the oil palm cultivars are DP Marihat, DP Bah Jambi, DP Sucfindo LaMe, DP Dolok Sinumbah and DP LAVROS.

In the jungle rubber plantation, two native trees, *E. zwageri* (EZ) and *A. scholaris* (AS), coexisted with the rubber trees. In this study, we use the term "native trees or forests" to refer to these two native tree species together. The native trees were about 20 meters tall, with a stem density of 525 ha^{-1}. Based on their Latin names, we use 'HBm' and 'HBj' to refer to rubber from the monoculture rubber plantation and jungle rubber plantation, respectively, while we use 'EG' to refer to oil palm. The trees *E. zwageri* and *A. scholaris* are referred to as EZ and AS, respectively. We also use 'OPP' and 'RP' to refer to oil palm plantation and rubber plantation, respectively, while we use 'JRP' to refer to jungle rubber plantation.

2.2. Sampling Procedure and Gas Exchange Measurements

We performed measurements on two trees or two palms that occurred close to the center of the 50 m × 50 m plot from 8th to 29th May 2017. The measurements were

conducted between 8:00 am and 2:00 pm local time. In the case of rubber and native trees, we selected a branch from the lower part of every tree and used a 5-meter ladder to access the branch. We assumed that at the lower part of the canopy, canopy bottoms are shade-prone, and thus all leaves are at least temporarily shaded. Two fully expanded matured leaves were identified per branch. Matured leaves were identified based on visual assessment of leaf color and size—this method has been used by Albert et al. [51].

CO_2 and H_2O gas exchanges were measured using a portable photosynthesis system (LI-6800; LiCor Biosciences, Lincoln, NE, USA) with a 3 × 3 cm^2 leaf chamber. The LI-6800 is an open gas exchange system, whereby the measurements of photosynthesis and transpiration are based on the differences in CO_2 and H_2O in an air stream that is entering (reference) and exiting the leaf (sample). The air stream flows through both the reference and sample gas analyzers and splits in the sensor head rather than the console, meaning that the conditioned air does not flow through two different tubes until the head. The head has a valve system that partitions the flow between the reference and sample gas analyzers. The valves also vent chamber air when matching the gas analyzers. It took about 20 minutes for the leaf to reach steady state conditions. Then, a light response curve was generated to determine the light saturation point (1500–1600 µmol photon m^{-2} s^{-1}). After the completion of the light response curve, we again allowed about 20 minutes for the same leaf to reach steady state conditions. Next, a CO_2 response curve on the same leaf was generated. Response curves of net photosynthesis (gross photosynthesis minus respiration, A_{net}) versus C_i (A_{net}/C_i), where C_i is the CO_2 concentration inside the leaf, and net photosynthesis versus photosynthetically active radiation (Q_{in}) (A_{net}/Q_{in}), was determined on four leaves from the same branch during each measurement period. For the A_{net}/C_i curves, leaves were acclimated in the chamber for about 10 minutes until A_{net} did not change over time. The A_{net}/C_i curves measurements were performed at a leaf temperature of 25 °C, a relative humidity of 70% and a photosynthetically active radiation of 1500 µmol photon m^{-2} s^{-1} in all cases. The CO_2 response curve (A_{net}/C_i) was then initiated with eight levels of CO_2 (400, 200, 0, 400, 600, 800, 1000 and 1200 µmol CO_2 mol^{-1} air). After completing the A_{net}/C_i curve, CO_2 concentration was kept constant at 400 µmol mol^{-1} air, and Q_{in} was sequentially lowered from 1500 to 1300, 1100, 900, 700, 500, 300, 100 and 0 µmol photon m^{-2} s^{-1}. We completed all of the CO_2 response curves and then performed the light response curves. Because photosynthesis has diurnal patterns e.g., [52], we ensured that am and pm measurements were equally represented.

In the case of oil palm, we selected a matured frond from the lower part of every palm and like in the case of trees, we used a 5-meter ladder to access the frond. Two fully matured leaf-lets from the center of the frond were identified per frond. As for trees, it took about 20 minutes for a leaf-let to reach steady state conditions. Next, a light response curve was generated to determine the light saturation point (1500–1600 µmol photon m^{-2} s^{-1}). After the completion of the light response curve, we allowed 20 minutes for the same leaf to reach steady state conditions. Finally, a CO_2 response curve on the same leaf-let was generated. We completed all of the CO_2 response curves and then performed the light response curves by following the similar protocol as for trees. Like for trees, we ensured that am and pm measurements for oil palms were equally represented. We also performed measurements on juvenile (young) trees/palms of all species. However, these young trees/palms were 'parasiting' under the planted canopy, instead of being planted on clearings left by missing adult trees, and therefore we did not consider comparing those data-sets with those used in the present study.

2.3. Response Curve Analyses

The estimates of V_{cmax25}, J_{max25}, and R_d were generated for the A/C_i curves by fitting the FvCB model [13,53] using the Plantecophys R package [54]. The general form of FvCB model used is expressed as

$$A_{net} = \min(A_c, A_j) - R_d, \quad (1)$$

where A_{net} is the net rate of CO_2 assimilation, A_c is the gross photosynthesis rate when Rubisco activity is limiting, A_j when RuBP-regeneration is limiting and R_d the rate of dark respiration. A_c and A_j are non-linear functions of the chloroplastic CO_2 concentration (C_c), both of the form k_1 ($C_c\Gamma^*$)/(k_2+C_c), where Γ^* is the CO_2 compensation point without R_d, and k_1 and k_2 are different parameter combinations for A_c and A_j. For a detailed description of these functions and the various parameters' temperature dependence, readers are referred to Medlyn et al. [55]. We used the default settings of the fitaci function from the Plantecophys package but provided the values of CO_2 concentration in the cuvette (CO_2S), C_i, leaf temperature, net photosynthesis, photosynthetically active radiation as an input. The fitaci function fits the FvCB model using the hyperbolic minimum of A_c and A_j, yielding estimates of V_{cmax}, J_{max}, and R_d and their standard errors. The hyperbolic minimum of A_c and A_j is described by:

$$A_m = \frac{A_c + A_j - \sqrt{(A_c + A_j)^2 - 4\theta A_c A_j}}{2\theta} - R_d, \quad (2)$$

where θ is a shape parameter, set to 0.99, and A_m is the hyperbolic minimum of A_c and A_j.

The response of A_{net} to Q_{in} was fitted to the non-rectangular hyperbolic function [56] described as

$$\theta(A_{net} + R_d)^2 - (\varepsilon Q_{in} + A_{max})(A_{net} + R_d) + \varepsilon Q_{in} A_{max} = 0, \quad (3)$$

from which A_{net} is calculated as

$$A_{net} = \frac{\varepsilon Q_{in} + A_{max} - \sqrt{(\varepsilon Q_{in} + A_{max})^2 - 4\theta\varepsilon Q_{in} A_{max}}}{2\theta} + R_d, \quad (4)$$

where A_{max} is the maximum rate of photosynthesis at saturating irradiance, R_d is the rate of respiration in the dark, θ defines the convexity of the response curve, and ε, the initial slope of the curve, is the photosynthetic light-use efficiency.

2.4. Leaf Nutrient Status and Specific Leaf Area

Following the gas exchange measurements, the same leaves were taken as samples in a dry paper envelope. The specific leaf area (*SLA*) was measured by cutting a disk with a size of 11.34 cm^2, then using a ratio of cut-area dry weight to total dry weight from the laboratory—a method that we adopted from Norby et al. [57]. This study refers to the inverse of *SLA* as the leaf mass per area ratio (*LMA*). The sampled leaves were dried for 72 h at 60 °C in an oven. The leaf carbon and nitrogen concentrations were analyzed using a CN analyzer (Vario EL Cube; Elementar Analysis Systems GmbH, Hanau, Germany). Leaf phosphorus, potassium and other element concentrations (e.g., Sulphur, Calcium, etc.) were determined by pressure digestion with concentrated HNO_3, and the digests were analyzed using inductively coupled plasma atomic emission spectrometry (iCAP 6300 Duo VIEW ICP Spectrometer, Thermo Fischer Scientific GmbH, Dreieich, Germany).

To keep it simple, in this study we followed Norby et al.'s [57] approach in determining the leaf nutrient contents. Norby et al. [57] also performed measurements in a tropical setting. We acknowledge that measurements on leaf chlorophyll or chlorophyll ratios might have provided further insights. These measurements could be a valuable direction for future research—where we compare and contrast strengths and weaknesses of the various methods used to derive leaf contents.

2.5. Theory for Within-Canopy Gradients in Photosynthetic Capacity

Generally, plant canopies have vertical gradients in physiological processes that relates to maximum carboxylation rates (V_{cmax25}), maximum light-saturated photosynthetic rates (A_{max}), area-based leaf nitrogen content (N_a) and *LMA* [58,59]. Canopy models often decrease leaf photosynthetic capacity with depth in the canopy using an exponential profile

of leaf nitrogen content [25,40,41]. In land surface models (e.g., CLM4) [25], V_{cmax25} is specified at the canopy top and is scaled with depth using the function

$$V_{cmax}(LAI) = V_{cmax25\_top} exp(-K_n LAI), \quad (5)$$

where LAI is the cumulative leaf area index and K_n is the extinction coefficient for V_{cmax}. A relatively high K_n value indicates a more rapid extinction of solar radiation than a relatively low K_n value, and implies a steeper decline in photosynthetic capacity through the canopy with respect to the leaf area index (LAI) [25]. This exponential saturation model does not consider some of the processes that could improve the scaled up estimate. First, it does not consider variations in leaf lifetimes [60], leaf angles and size [61,62] along the vertical canopy profile. Second, the method does not consider individual tree heights [63,64] and within- and between-species variations in nutrient concentrations [65]. Third, it does not include effects of direct versus diffuse radiation [66]. Finally, although the decline in photosynthetically critical elements such as nitrogen and phosphorus with increasing depth in plant canopies can be considerable, this decline may be never to the same extent that it matches the reduction in radiation with canopy depth [67,68]. However, the scaling up algorithm has been successfully applied in a number of studies [65,69–71], so by combining 'isolated dataset for only one stratum' from this study with 'K_n' estimates from previous studies, we are able to present a model that is more conceptual rather than quantitative, and can be used for the parameterization of the gas exchange when developing models for CO_2 exchange in tropical settings. The maximum electron transport rate (J_{max_top}), leaf respiration rate ($R_{\mathrm{d\_top}}$), and other photosynthetic parameters (A_{max_top}, $LMA_{\mathrm{\_top}}$, $N_{\mathrm{a\_top}}$) at the top of the canopy are similarly scaled with canopy depth. Using previous studies, we estimate K_n values for our oil palm plantation, rubber plantation and jungle rubber plantation canopies (see in Appendix A for details).

2.6. Measured Data-Sets

LAI measurements were performed in May until mid-June 2018 at five locations in five subplots (a total of 25 measurements per land-use type (or per plantation plot)) in a 50 m × 50 m plot using the LAI-2200 plant canopy analyzer (LiCOR, Biosciences, Lincoln, NE, USA). We placed the LAI-2200 plant canopy analyzer in different positions so as to capture the spatial heterogeneity, and these 25 measurements were representative of the plant community. The measurements were conducted in oil palm plantation, rubber plantation, jungle rubber plantation and forests on sunny days (see in Appendix B for further details). To compare our up-scaled estimate of leaf mass per area and leaf nitrogen content at the top of the canopy with measurements, we obtained measured data from Kotowska et al. [43], which was measured at the same site and on a similar plant age.

2.7. Scaling Up Photosynthetic Capacity and Data Availability

After 'K_n' values were estimated for every land-use type, we use 'inversion technique' to estimate the photosynthetic capacity at the top of the canopy. Basically, we inverted Equation (5), wherein

$$V_{cmax25\_top} = V_{cmax}(LAI)/exp(-K_n LAI), \quad (6)$$

The maximum electron transport rate (J_{max_top}), leaf respiration rate ($R_{\mathrm{d\_top}}$) and other photosynthetic parameters (A_{max_top}, $LMA_{\mathrm{\_top}}$, $N_{\mathrm{a\_top}}$) at the top of the canopy are similarly scaled with canopy depth (see in Appendix C for further details). All of the original data set related to photosynthetic capacity is publicly available through https://github.com/ashehad/Photosynthetic_capacity_tropics/ (access on 16 February 2021).

A summarized version of the data can be also found in the same repository. To show what the scaling of photosynthetic capacity means to the land surface models (e.g., CLM5) [72,73], as an example, we obtained the baseline (default) values of maximum carboxylation rate (V_{cmax_top}) and $N_{\mathrm{a\_top}}$ from CLM5 for tropical evergreen forests and

compared it with the values of maximum carboxylation rate (V_{cmax_top}) and N_{a_top} using the scaling method applied in this study for a potential tropical evergreen forest.

3. Results

3.1. Variation of Photosynthetic Capacity at the Lower Part of the Canopy

Values of V_{cmax25} ranged from 5.7 to 47 µmol CO_2 m^{-2} s^{-1} among all species (Figure 1a) at the lower part of the canopy. HBm and HBi species exhibited the highest values of V_{cmax25} (Figure 1a), while EZ species had the lowest values (Figure 1a)—a similar trend was noted for J_{max25} (Figure 1b). Values of J_{max25} ranged from 16 to 10.7 µmol electron m^{-2} s^{-1} among all species (Figure 1b) at the lower part of the canopy. No considerable difference in leaf nitrogen content (N_a) values was found among EG, HBm and HBj species (Figure 1c). EZ species had the lowest N_a values (Figure 1c). N_a values ranged from 0.74 to 1.49 g N m^{-2} among all species (Figure 1c).

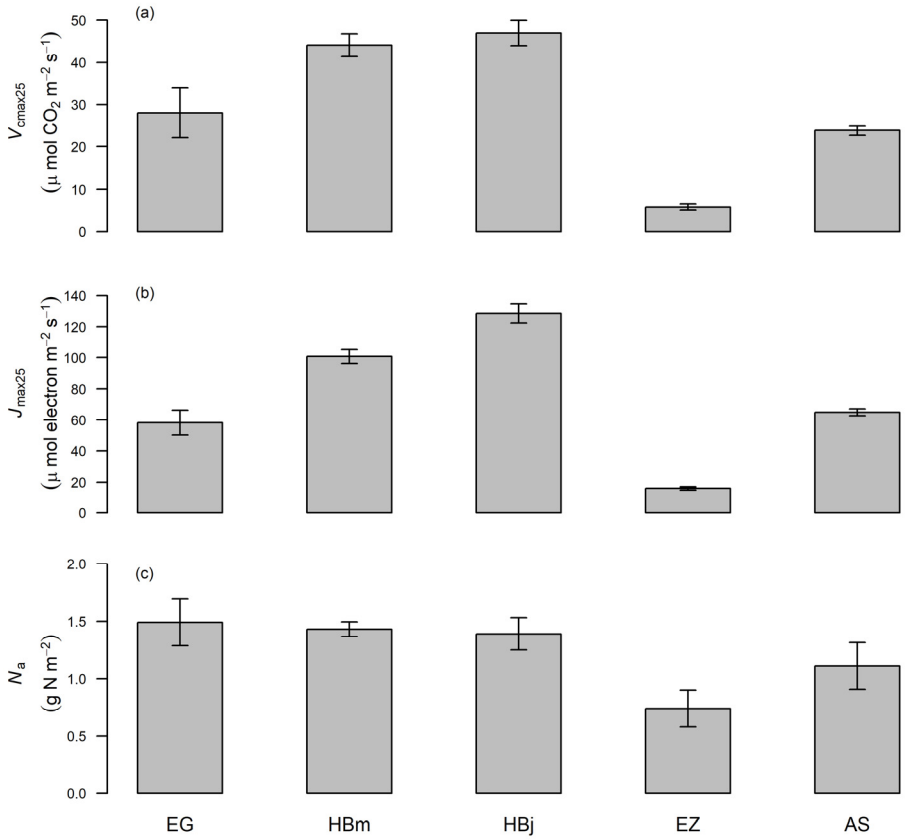

Figure 1. Mean (with standard error bars, n = 4) maximum carboxylation capacity (V_{cmax25}, (**a**)), maximum electron transport rate (J_{max25}, (**b**)) and leaf nitrogen content (N_a) (**c**) of leaves of monoculture oil palm (EG), monoculture rubber tree (HBm), jungle rubber tree (HBj), and two native tree species (EZ and AS) measured at the lower part of the canopy. The data included mature oil palm and mature trees.

AS species had the highest values of A_{max} (Figure 2a). Overall, species' means of A_{max} varied more than four-fold (from 3.2 to 13.3 µmol CO_2 m^{-2} s^{-1}) (Figure 2a). Within species, R_d varied much more than A_{max} (Figure 1a,b). The species' R_d values ranged from 0.2 to 1.31 µmol CO_2 m^{-2} s^{-1} (Figure 2b) at the lower part of the canopy. EZ species had the least R_d and *LMA* values (Figure 2b,c). Among species, low- and high-*LMA* values were 29 and 61.5 g m^{-2}, respectively (Figure 2c).

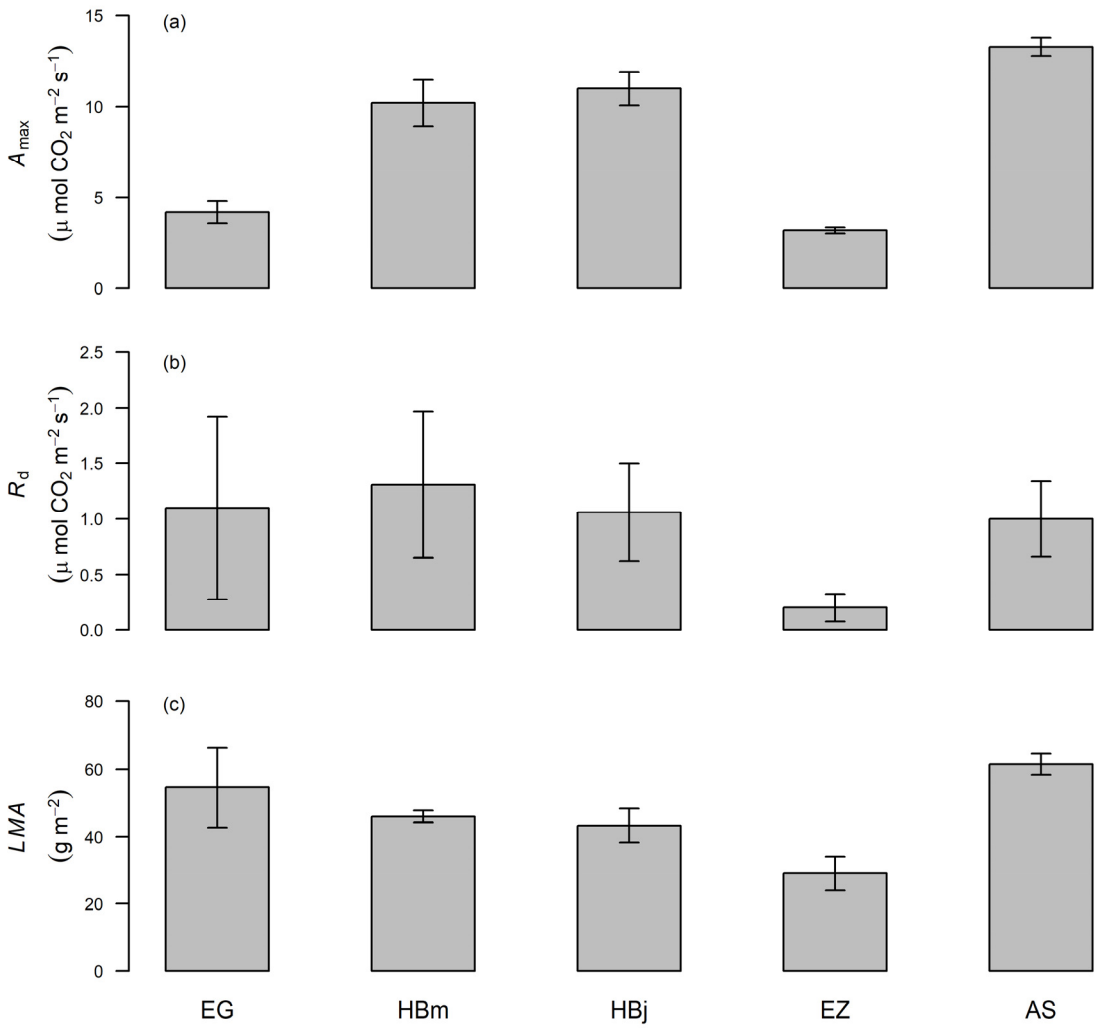

Figure 2. Mean (with standard error bars, n = 4) light-saturated net photosynthesis (A_{max}, (**a**)), non-photorespiratory respiration (R_d, (**b**)) and leaf mass per area ratio (*LMA*) (**c**) of leaves of monoculture oil palm (EG), monoculture rubber tree (HBm), jungle rubber tree (HBj), and two native tree species (EZ and AS) measured at the lower part of the canopy. The data included matured oil palm and matured trees.

3.2. Extinction of Light in the Canopy Profile

Oil palm plantation (OPP) had the highest K_n value (0.32 m^2 m^{-2}; Figure 3a), while rubber and jungle plantation had similar K_n values (~0.2 m^2 m^{-2}; Figure 3a). The jungle rubber plantation had the highest *LAI* value (*LAI* = 5.3 m^2 m^{-2}; Figure 3b) while oil palm plantation exhibited moderate *LAI* value (*LAI* = 2.8 m^2 m^{-2}; Figure 3b). The rubber monoculture plantation had the least *LAI* value (*LAI* = 2.3 m^2 m^{-2}; Figure 3b).

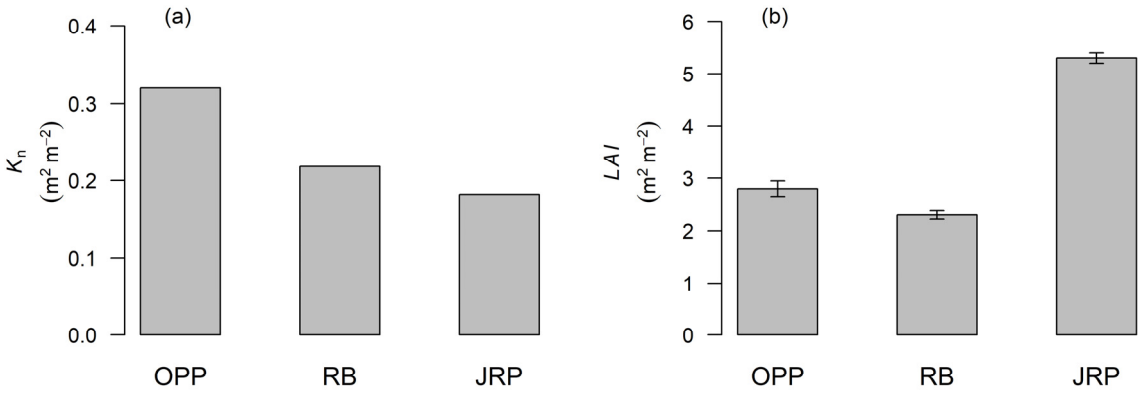

Figure 3. Estimates of light penetration in the canopy ('K_n', (**a**)) in oil palm plantation (OPP), rubber plantation (RB) and jungle rubber plantation (JRP). A relatively high K_n value indicates a more rapid extinction of light than a relatively low K_n value and implies a steeper decline in photosynthetic capacity through the canopy with respect to the leaf area index (*LAI*). Measured values of *LAI* (**b**) in OPP, RB and JRP.

3.3. Variation of Photosynthetic Capacity at the Top of the Canopy

OPP, RP and JRP exhibited similar V_{cmax25} values at the top of the canopy (~69.4 µmol CO_2 m^{-2} s^{-1}; Figure 4a)), while values of J_{max25} at the top of canopy ranged from 142 to 183 µmol electron m^{-2} s^{-1} among these three plantations (Figure 4b). At the top of the canopy, the J_{max25}: V_{cmax25} ratio ranged from 2.1 to 2.7 µmol electron μmol^{-1} CO_2 among all the three plantations (Figure 4a,b), wherein both OPP and RP had a lower J_{max25}: V_{cmax25} ratio than the JRP (Figure 4a,b).

At the top of the canopy, A_{max} varied considerably among different plantations (10.3 to 24.1 µmol CO_2 m^{-2} s^{-1}; Figure 4c), JRP had the highest values of A_{max} (24.1 µmol CO_2 m^{-2} s^{-1}; Figure 4c) and the OPP had the lowest values (10.3 µmol CO_2 m^{-2} s^{-1}; Figure 4c)—a similar trend was observed for J_{max25} at the top of the canopy (Figure 4b). Like in the case of V_{cmax25}, there were similar R_d values at the top of the canopy (~2.3 µmol CO_2 m^{-2} s^{-1}; Figure 4d)).

3.4. Area-Based Leaf Nitrogen Content and Leaf Mass Per Area

At the top of the canopy, the scaling method used in this study estimated the largest N_a value for the OPP, while it estimated the least for the RP and JRP (3.6 versus ~2.6 g N m^{-2}; Figure 5a). For the OPP, the estimated N_a value at the top of the canopy via the scaling method was underestimated compared to the field measurements (3.6 versus 5.6 g N m^{-2}; Figure 5a). However, there were little differences in N_a values at the top of the canopy between the scaling method and measurements for RP and JRP (Figure 5a).

In line with the field measurements, the scaling method used in this study estimated the highest value of *LMA* at the top of the canopy for the OPP (133.5 g m^{-2}; Figure 5a). There was a considerable difference in *LMA* values at the top of the canopy between the scaling method and measurements for JRP (117 versus 94 g m^{-2}; Figure 5b).

From the lower part of the canopy to the top, N_a values increased from 1.5 to 3.7 g N m^{-2} in OPP, whereas N_a values increased from 1.43 to 2.36 g N m^{-2} in RB (Figure 1c, Figure 5a). In the case of *LMA*, from the lower part of the canopy to the top, its values increased from 54.5 to 133.5 g m^{-2}, whereas *LMA* values increased from 45.9 to 75.8 g m^{-2} in RB (Figure 2c, Figure 5b).

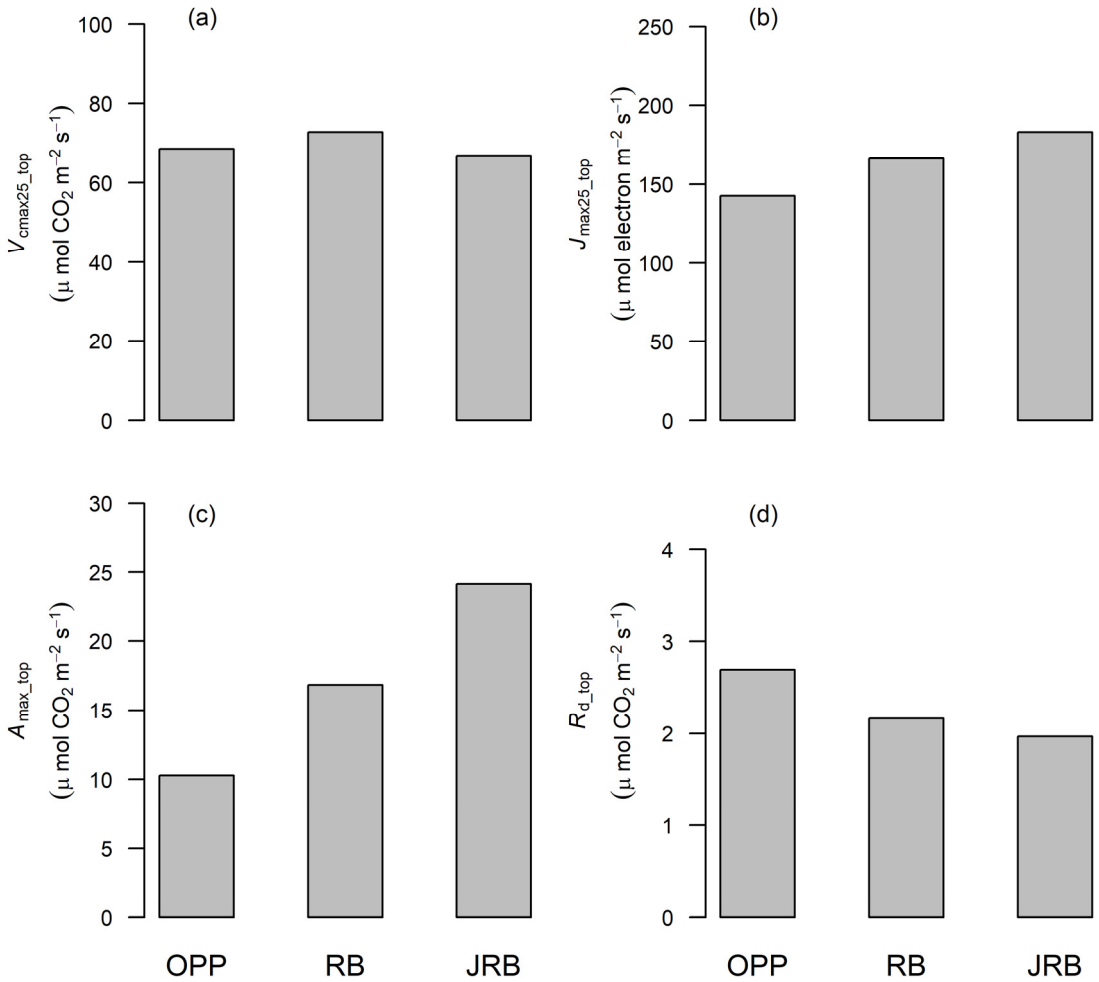

Figure 4. Photosynthetic traits (V_{cmax25_top}; (**a**), J_{max25_top}; (**b**), A_{max_top}; (**c**), R_{d_top}, (**d**)) estimated at the top of the canopy via the scaling method in OPP, RB and JRP.

3.5. Within-Canopy Gradients for Forest Ecosystems

Forests had the lowest K_n value (0.15 m^2 m^{-2}) compared to oil palm plantations, rubber plantations and jungle rubber plantations (Figure 3a). On the contrary, forests had the highest leaf area index value (6 m^2 m^{-2}) compared to oil palm plantations, rubber plantations and jungle rubber plantations (Figure 3b). The N_a: V_{cmax25_top} ratio using the scaling method is higher than the default CLM5 model (0.064 versus 0.05 g N s/μmol CO_2).

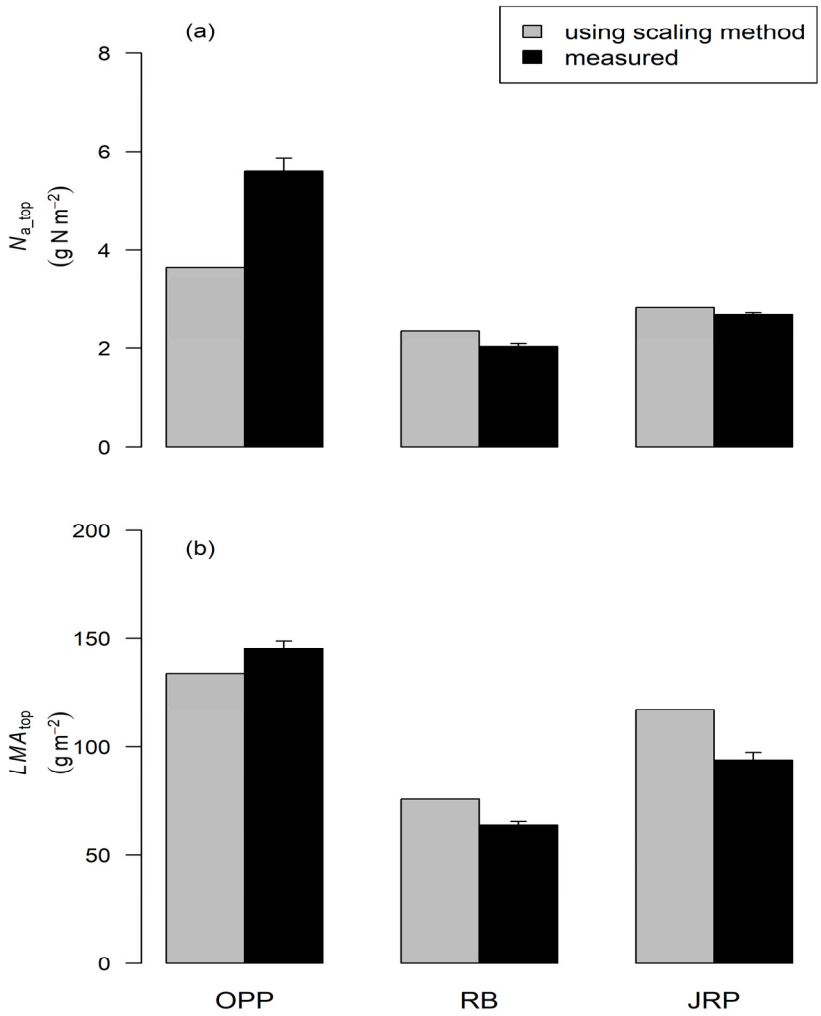

Figure 5. Comparison of leaf nitrogen content ((**a**), N_{a_top}) and leaf mass per area ((**b**), LMA_{top}) estimated at the top of the canopy via the scaling method with the measured values in OPP, RB and JRP.

4. Discussion

4.1. Interspecific Variability in Photosynthetic Traits at the Bottom of the Canopy

In our study, the high V_{cmax25} values for *H. brasiliensis* from monoculture rubber plantation or jungle rubber plantation can be due to a high area-based leaf nitrogen content (Figure 1c). It is worth noting that for the *H. brasiliensis* from monoculture rubber plantation or jungle rubber plantation, our measured value of V_{cmax25} (~45 µmol CO_2 m^{-2} s^{-1}) is higher than the value reported by Kumagai et al. [74], who observed V_{cmax25} values of 30 µmol CO_2 m^{-2} s^{-1} at the bottom of the canopy. The difference in V_{cmax25} can be linked to differences in *LAI*, where our studied rubber plantation had much lower *LAI* than that of Kumagai et al. [74] (2.3 m^2 m^{-2} versus 3.89 m^2 m $^{-2}$). A low *LAI* could mean a high canopy openness, more light penetration, and thus a high V_{cmax25} at the lower part of the canopy. The relatively low value of A_{max} (4.2 µmol CO_2 m^{-2} s^{-1}) for *E. guineensis* from oil palm plantation at the bottom of the canopy is due to a lower value of V_{cmax25} and J_{max25} (Figure 1a,b) and a relatively high R_d value (Figure 2b).

4.2. Light Extinction in the Canopy Profile

The high K_n value in oil palm plantation suggests that a relatively large amount of light is extinct in the oil palm plantation compared to monoculture rubber plantation or jungle rubber plantation. Subsequently, from the top to the lower part of the canopy, photosynthetic capacity declines faster in oil palm plantation than monoculture rubber plantation or jungle rubber plantation. Our estimate of K_n for forests (0.15 m^2 m^{-2}) is in

agreement with the values from Kattge et al. [24] that showed variations from 0.13 to 0.23. The K_n value for forests in this study is also closer to Bonan et al. [25] (0.11 m^2 m^{-2}), who derived it from observations.

In general, the light extinction approach is more valid for spatially uniform plant canopy than non-uniform plant canopy, as non-uniform plant canopy is usually characterized by a mosaic solar radiation pattern [75,76]. Therefore, for non-uniform plant canopies, we posit that there could be uncertainties associated with estimating the photosynthesis parameters at the top of the canopy using the up-scaling procedure used in this study.

4.3. Photosynthetic Trait Variability at the Top of the Canopy

The value of V_{cmax25} estimated by the scaling method for *E. guineensis* at the top of the canopy (V_{cmax25} = 69 µmol CO_2 m^{-2} s^{-1}) is similar to those reported by Rival [77] (V_{cmax25} = 74 µmol CO_2 m^{-2} s^{-1}). For the monoculture rubber plantation, our estimate of V_{cmax25} at the top of the canopy (V_{cmax25} = 73 ± µmol CO_2 m^{-2} s^{-1}) is closer to the value reported by Kumagai et al. [74], who observed V_{cmax25} values of 70 µmol CO_2 m^{-2} s^{-1}. Our estimate of V_{cmax25} at the top of the canopy for a potential forest ecosystem that consist of the two native tree species (V_{cmax25} = 36 µmol CO_2 m^{-2} s^{-1}) is comparable with values reported from other tropical forest sites [28,78,79]. Overall, the higher V_{cmax25} and J_{max25} of rubber trees and oil palms compared to the forest ecosystem that consist of the two native tree species were in line with the findings of Leuning et al. [80], who reported that these photosynthetic capacity parameters are more commonly higher in agricultural than non-agricultural species.

In our study, the estimate of A_{max} of *H. brasiliensis* in the monoculture rubber plantation at the top of the canopy was 16.8 µmol CO_2 m^{-2} s^{-1}—this value is slightly higher than the value (A_{max} = 13.1 µmol CO_2 m^{-2} s^{-1}) reported on two-year-old rubber seedlings grown in the field [81]. In the case of *E. guineensis*, the estimate of A_{max} at the top of the canopy was 10.3 µmol CO_2 m^{-2} s^{-1}, which is slightly lower than Corley [82] (A_{max} = 14 µmol CO_2 m^{-2} s^{-1}).

The scaling method estimated the highest value of A_{max} (24.1 µmol CO_2 m^{-2} s^{-1}) in the jungle rubber plantation at the top of the canopy. The reason for this is due to a relatively high leaf nitrogen content (Figure 5a); this reason is also supported by the measurements from the top of the canopy (Figure 5a) [43].

4.4. Limitations and Implications of Scaling Method Used in This Study

In this study, we did not perform diurnal integrative assessments of the light environment. This is important especially for studying diurnal patterns of photosynthesis, looking at diurnal shading patterns and investigating the inhibition of photosynthesis, e.g., [83]. Our up-scaled values of photosynthetic capacity related traits from the lower part of the canopy to the top of the canopy suffer from a couple of shortcomings. First, we used the leaf area index estimates from the similar month, but from a subsequent year. Second, we have studied only two native tree species from the jungle rubber plantation.

Our up-scaled values of photosynthetic capacity-related traits from the lower part of the canopy to the top of the canopy matched reasonably well with the previous measurements from our studied sites, e.g., [43] as well as from the literature [74,77]. This indicates that our data can be integrated with the land surface models (e.g., CLM5) [72,73]. As an example, for a potential tropical evergreen forest ecosystem, our estimated N_a: V_{cmax25_top} ratio using the scaling method was higher than the default CLM5 [72,73] model because mainly the area-based leaf nitrogen content at the top of the canopy was 30% higher, as a result of the scaling method than the default CLM5. It is worth noting that measurements at our study sites indicate a 2-fold area-based leaf nitrogen content at the top of the canopy compared to the default CLM5. The high N_a: V_{cmax25_top} ratio suggests that if CLM5 is parameterized with our estimates from the scaling method, the transpiration estimate of CLM5 will have greater sensitivity than the default CLM5. We do acknowledge, however, that the transpiration estimate of CLM5 is also sensitive to other parameters, such as the stomatal slope that relates stomatal conductance to photosynthesis [73].

5. Conclusions

We can conclude that the photosynthetic capacity-related traits measured at the lower part of the canopy can be successfully scaled up to the top of the canopy, especially for closed and uniform plant canopies. Future measurement efforts for species studied in this study should focus on upper canopy locations, so that our study's data-sets can be combined and the variability of leaf traits in the vertical canopy profile can be investigated.

Author Contributions: A.A.A., B.I., E.V. and A.K. designed the experiment. B.N. and A.A.A. performed the experiments. B.N., A.A.A. and A.K. analyzed the data, and took part in the initial writing of the manuscript. All authors contributed to writing the final version of the manuscript. All authors have read and agreed to the published version of the manuscript.

Funding: We gratefully acknowledge financial supports from the Deutsche Forschungsgemeinschaft (DFG, German Research Foundation)—project number 192626868—SFB 990 and the Ministry of Research, Technology and Higher Education (Ristekdikti) in the framework of the collaborative German-Indonesian research project CRC990 in the subproject A07.

Institutional Review Board Statement: Not Applicable.

Informed Consent Statement: Not Applicable.

Data Availability Statement: The data presented in this study are openly available at https://github.com/ashehad/Photosynthetic_capacity_tropics/ (accessed on17 March 2021).

Acknowledgments: We thank George Ofori Ankomah from the University of Goettingen for measuring the leaf area index at the studied rubber plantations. Finally, we thank the village leaders and farmers for allowing us to conduct our research on their land.

Conflicts of Interest: The authors declare no conflict of interest.

Appendix A. Estimating K_n Values of Plantations

In a large-scale commercial oil palm plantation (LSCOPP) in Jambi, where Meijide et al. [84] measured V_{cmax25} in the vertical canopy profile, where the V_{cmax25} value at the bottom was 13.1 µmol CO_2 m^{-2} s^{-1}, while at the top of the canopy it was 42 µmol CO_2 m^{-2} s^{-1}. Since the leaf area index at LSCOPP has been 3.64 m^2 m^{-2} [85,86], we have

$$V_{cmax}(LAI) = V_{cmax25\_top} exp(-K_n LAI), \tag{A1}$$

Substituting the known values in Equation (A1) results in

$$13.1 = 42 * exp(-K_n 3.64), \tag{A2}$$

from which K_n value can be determined for the LSCOPP. We assume that the estimate of 'K_n' at LSOPP will be similar at our studied oil palm plantation site.

For the rubber plantation site (RPC) in Cambodia, where Kumagai et al. [74] measured V_{cmax25} in the vertical canopy profile, where V_{cmax25} value at the bottom of the canopy was 30 µmol CO_2 m^{-2} s^{-1} while at the top of the canopy it was 70 µmol CO_2 m^{-2} s^{-1}. Since the leaf area index at the RPC is 3.89 m^2 m^{-2} [74], substituting the known values in Equation (A1) results in

$$30 = 70 * exp(-K_n 3.89), \tag{A3}$$

from which K_n value can be determined for the RPC. As for the oil palm plantation case, we assume that the estimate of 'K_n' at RPC will be similar at our studied rubber plantation site.

To determine 'K_n' values for forest site in Jambi, we used the value of V_{cmax25} (53 µmol CO_2 m^{-2} s^{-1}) as measured at the top of the canopy at a tropical forest site in Bariri, Indonesia [87] to calculate the value of 'K_n'. Lloyd et al. [59] analyzed many tropical forest canopies and found that the K_n value scales with $V_{\max 25}$ using the following relation

$$K_n = exp\left(0.00963 V_{cmax25\_top} - 2.43\right), \tag{A4}$$

where high values of K_n results in steeper declines in photosynthetic capacity through the canopy profile with respect to the cumulative leaf area index.

Finally, to estimate 'K_n' values for jungle rubber plantation, we summed the K_n values of forests and rubber plantation and then halved it.

Appendix B. Leaf Area Index Measurements

A 50 m × 50 m plot was established by the EFForTS project in oil palm plantation, rubber plantation, jungle rubber plantation and forest [42]. Each plot contained five subplots measuring 5 × 5 m, which was unevenly laid at specific locations. *LAI* measurements were conducted in May until mid-June 2018 at five positions in all five subplots established within each of the plantation plot using the LAI-2200 plant canopy analyzer. *LAI* data were obtained from above and below canopy readings taken simultaneously in each subplot with two LAI-2200 devices. All measurements were taken with view cap-free wands under diffused sky conditions. Optical sensors were covered and packed into its protective case at the slightest detection of precipitation to avoid any potential optical damage to the sensors and other sensitive parts of the device. Wands were always orientated towards the magnetic north with the use of a compass (LI-COR, Inc., Lincoln, NE, USA2017). The above canopy readings were captured by mounting a 10-second autolog wand (reference sensor) facing the sky on a 2 m sturdy tripod with an accurate leveling bubble. This was positioned in nearby open areas to the core plots of at least 200 m × 200 m range with surrounding vegetation height less than 3.5 m to ensure a sensor's view of the sky across a wide azimuth [88]. The below canopy readings in each plot were taken concurrently with that of the reference sensor at five positions within each subplot, to obtain accurate measurement of canopy transmission (LI-COR, Inc., 2017). The distance between designated reference sensor locations (open areas) and core plots for below canopy readings was less than 1 km, to ensure uniform sky brightness between the two-sensor locations for canopy measurements. *LAI* values for subplots were averaged out for the respective plantation plots.

Appendix C. Calculation of the Photosynthetic Capacity Using the Scaling Method

To estimate the value of V_{cmax25} at the top of the canopy (V_{cmax25_top}) at our studied oil palm plantation, we substituted the measured value of V_{cmax25} at the bottom of the canopy, and the derived value of K_n and the measured value of leaf area index at our studied oil palm plantation in the following equation:

$$V_{cmax25\_top} = V_{cmax25}/(exp(-K_n LAI)) \quad \text{(A5)}$$

A similar form of the equation was used to estimate values of J_{max25_top}, N_{a_top}, A_{max_top}, R_{d_top} and $LMA_{\_top}$.

For our studied rubber plantation site, we substituted the measured value of V_{cmax25} at the bottom of the canopy, and the derived value of K_n and the measured value of leaf area index at our studied rubber plantation in equation A5. We used a similar form of equation A5 as was used to estimate values of J_{max25_top}, N_{a_top}, A_{max_top}, R_{d_top} and $LMA_{\_top}$ for the rubber plantation.

Using a similar approach (as in above), we estimated values of V_{cmax25_top}, J_{max25_top}, N_{a_top}, A_{max_top}, R_{d_top} and $LMA_{\_top}$ for jungle rubber plantation by using its K_n value and the measured value of leaf area index. We also used a similar approach (as in above) to estimate values of V_{cmax25_top} and N_{a_top} for a potential tropical evergreen forest ecosystem by using its K_n value and the measured value of leaf area index. To determine the V_{cmax25} values at the lower part of the canopy for the potential tropical evergreen forest ecosystem, we summed the V_{cmax25} values of the two native tree species and then halved it. We followed the same method to obtain the N_a values at the lower part of the canopy for the potential tropical evergreen forest ecosystem.

References

1. Ziegler, A.D.; Phelps, J.; Yuen, J.Q.; Webb, E.L.; Lawrence, D.; Fox, J.M.; Bruun, T.B.; Leisz, S.J.; Ryan, C.M.; Dressler, W.; et al. Carbon Outcomes of Major Land-Cover Transitions in SE Asia: Great Uncertainties and REDD+ Policy Implications. *Glob. Chang. Biol.* **2012**, *18*, 3087–3099. [CrossRef]
2. Houghton, R.A.; House, J.I.; Pongratz, J.; van der Werf, G.R.; DeFries, R.S.; Hansen, M.C.; Quéré, C.L.; Ramankutty, N. Carbon Emissions from Land Use and Land-Cover Change. *Biogeosciences* **2012**, *9*, 5125–5142. [CrossRef]
3. Margono, B.A.; Turubanova, S.; Zhuravleva, I.; Potapov, P.; Tyukavina, A.; Baccini, A.; Goetz, S.; Hansen, M.C. Mapping and Monitoring Deforestation and Forest Degradation in Sumatra (Indonesia) Using Landsat Time Series Data Sets from 1990 to 2010. *Environ. Res. Lett.* **2012**, *7*, 034010. [CrossRef]
4. Clough, Y.; Krishna, V.V.; Corre, M.D.; Darras, K.; Denmead, L.H.; Meijide, A.; Moser, S.; Musshoff, O.; Steinebach, S.; Veldkamp, E.; et al. Land-Use Choices Follow Profitability at the Expense of Ecological Functions in Indonesian Smallholder Landscapes. *Nat. Commun.* **2016**, *7*, 13137. [CrossRef] [PubMed]
5. Luskin, M.S.; Christina, E.D.; Kelley, L.C.; Potts, M.D. Modern Hunting Practices and Wild Meat Trade in the Oil Palm Plantation-Dominated Landscapes of Sumatra, Indonesia. *Hum. Ecol.* **2014**, *42*, 35–45. [CrossRef]
6. Rist, L.; Feintrenie, L.; Levang, P. The Livelihood Impacts of Oil Palm: Smallholders in Indonesia. *Biodivers. Conserv.* **2010**, *19*, 1009–1024. [CrossRef]
7. Grass, I.; Kubitza, C.; Krishna, V.V.; Corre, M.D.; Mußhoff, O.; Pütz, P.; Drescher, J.; Rembold, K.; Ariyanti, E.S.; Barnes, A.D.; et al. Trade-Offs between Multifunctionality and Profit in Tropical Smallholder Landscapes. *Nat. Commun.* **2020**, *11*, 1186. [CrossRef] [PubMed]
8. van Straaten, O.; Corre, M.D.; Wolf, K.; Tchienkoua, M.; Cuellar, E.; Matthews, R.B.; Veldkamp, E. Conversion of Lowland Tropical Forests to Tree Cash Crop Plantations Loses up to One-Half of Stored Soil Organic Carbon. *Proc. Natl. Acad. Sci. USA* **2015**, *112*, 9956–9960. [CrossRef]
9. Kotowska, M.M.; Leuschner, C.; Triadiati, T.; Meriem, S.; Hertel, D. Quantifying Above- and Belowground Biomass Carbon Loss with Forest Conversion in Tropical Lowlands of Sumatra (Indonesia). *Glob. Chang. Biol.* **2015**, *21*, 3620–3634. [CrossRef]
10. Guillaume, T.; Kotowska, M.M.; Hertel, D.; Knohl, A.; Krashevska, V.; Murtilaksono, K.; Scheu, S.; Kuzyakov, Y. Carbon Costs and Benefits of Indonesian Rainforest Conversion to Plantations. *Nat. Commun.* **2018**, *9*, 2388. [CrossRef]
11. Allen, K.; Corre, M.D.; Tjoa, A.; Veldkamp, E. Soil Nitrogen-Cycling Responses to Conversion of Lowland Forests to Oil Palm and Rubber Plantations in Sumatra, Indonesia. *PLoS ONE* **2015**, *10*, e0133325. [CrossRef] [PubMed]
12. Hassler, E.; Corre, M.D.; Tjoa, A.; Damris, M.; Utami, S.R.; Veldkamp, E. Soil Fertility Controls Soil–Atmosphere Carbon Dioxide and Methane Fluxes in a Tropical Landscape Converted from Lowland Forest to Rubber and Oil Palm Plantations. *Biogeosciences* **2015**, *12*, 5831–5852. [CrossRef]
13. Farquhar, G.D.; von Caemmerer, S.; Berry, J.A. A Biochemical Model of Photosynthetic CO2 Assimilation in Leaves of C3 Species. *Planta* **1980**, *149*, 78–90. [CrossRef] [PubMed]
14. Ball, J.T.; Woodrow, I.E.; Berry, J.A. A Model Predicting Stomatal Conductance and its Contribution to the Control of Photosynthesis under Different Environmental Conditions. In *Progress in Photosynthesis Research: Volume 4, Proceedings of the VIIth International Congress on Photosynthesis Providence, Rhode Island, USA, 10–15 August 1986*; Biggins, J., Ed.; Springer: Dordrecht, The Netherlands, 1987; pp. 221–224. ISBN 978-94-017-0519-6.
15. Sharkey, T.D.; Bernacchi, C.J.; Farquhar, G.D.; Singsaas, E.L. Fitting Photosynthetic Carbon Dioxide Response Curves for C3 Leaves. *Plant Cell Environ.* **2007**, *30*, 1035–1040. [CrossRef]
16. Kumarathunge, D.P.; Medlyn, B.E.; Drake, J.E.; Rogers, A.; Tjoelker, M.G. No Evidence for Triose Phosphate Limitation of Light-Saturated Leaf Photosynthesis under Current Atmospheric CO2 Concentration. *Plant Cell Environ.* **2019**. [CrossRef]
17. Stefanski, A.; Bermudez, R.; Sendall, K.M.; Montgomery, R.A.; Reich, P.B. Surprising Lack of Sensitivity of Biochemical Limitation of Photosynthesis of Nine Tree Species to Open-Air Experimental Warming and Reduced Rainfall in a Southern Boreal Forest. *Glob. Chang. Biol.* **2019**. [CrossRef]
18. Rogers, A.; Medlyn, B.E.; Dukes, J.S.; Bonan, G.; von Caemmerer, S.; Dietze, M.C.; Kattge, J.; Leakey, A.D.B.; Mercado, L.M.; Niinemets, Ü.; et al. A Roadmap for Improving the Representation of Photosynthesis in Earth System Models. *New Phytol.* **2017**, *213*, 22–42. [CrossRef] [PubMed]
19. Lombardozzi, D.L.; Smith, N.G.; Cheng, S.J.; Dukes, J.S.; Sharkey, T.D.; Rogers, A.; Fisher, R.; Bonan, G.B. Triose Phosphate Limitation in Photosynthesis Models Reduces Leaf Photosynthesis and Global Terrestrial Carbon Storage. *Environ. Res. Lett.* **2018**, *13*, 074025. [CrossRef]
20. Ellsworth, D.S.; Crous, K.Y.; Lambers, H.; Cooke, J. Phosphorus Recycling in Photorespiration Maintains High Photosynthetic Capacity in Woody Species. *Plant Cell Environ.* **2015**, *38*, 1142–1156. [CrossRef]
21. Wullschleger, S.D. Biochemical Limitations to Carbon Assimilation in C3 Plants—A Retrospective Analysis of the A/Ci Curves from 109 Species. *J. Exp. Bot.* **1993**, *44*, 907–920. [CrossRef]
22. Medlyn, B.E.; Badeck, F.-W.; De Pury, D.G.G.; Barton, C.V.M.; Broadmeadow, M.; Ceulemans, R.; Angelis, P.D.; Forstreuter, M.; Jach, M.E.; Kellomäki, S.; et al. Effects of Elevated [CO_2] on Photosynthesis in European Forest Species: A Meta-Analysis of Model Parameters. *Plant Cell Environ.* **1999**, *22*, 1475–1495. [CrossRef]
23. Bonan, G.B.; Levis, S.; Sitch, S.; Vertenstein, M.; Oleson, K.W. A Dynamic Global Vegetation Model for Use with Climate Models: Concepts and Description of Simulated Vegetation Dynamics. *Glob. Chang. Biol.* **2003**, *9*, 1543–1566. [CrossRef]

24. Kattge, J.; Knorr, W.; Raddatz, T.; Wirth, C. Quantifying Photosynthetic Capacity and Its Relationship to Leaf Nitrogen Content for Global-Scale Terrestrial Biosphere Models. *Glob. Chang. Biol.* **2009**, *15*, 976–991. [CrossRef]
25. Bonan, G.B.; Lawrence, P.J.; Oleson, K.W.; Levis, S.; Jung, M.; Reichstein, M.; Lawrence, D.M.; Swenson, S.C. Improving Canopy Processes in the Community Land Model Version 4 (CLM4) Using Global Flux Fields Empirically Inferred from FLUXNET Data. *J. Geophys. Res. Biogeosciences* **2011**, *116*. [CrossRef]
26. Rogers, A. The Use and Misuse of V(c,Max) in Earth System Models. *Photosyn. Res.* **2014**, *119*, 15–29. [CrossRef] [PubMed]
27. Thomas, S.C.; Winner, W.E. Photosynthetic Differences between Saplings and Adult Trees: An Integration of Field Results by Meta-Analysis. *Tree Physiol.* **2002**, *22*, 117–127. [CrossRef] [PubMed]
28. Coste, S.; Roggy, J.-C.; Imbert, P.; Born, C.; Bonal, D.; Dreyer, E. Leaf Photosynthetic Traits of 14 Tropical Rain Forest Species in Relation to Leaf Nitrogen Concentration and Shade Tolerance. *Tree Physiol.* **2005**, *25*, 1127–1137. [CrossRef]
29. Vincent, G. Leaf Life Span Plasticity in Tropical Seedlings Grown under Contrasting Light Regimes. *Ann. Bot.* **2006**, *97*, 245–255. [CrossRef]
30. Reich, P.B.; Oleksyn, J.; Wright, I.J. Leaf Phosphorus Influences the Photosynthesis-Nitrogen Relation: A Cross-Biome Analysis of 314 Species. *Oecologia* **2009**, *160*, 207–212. [CrossRef]
31. Ely, K.S.; Rogers, A.; Agarwal, D.A.; Ainsworth, E.A.; Albert, L.P.; Ali, A.; Anderson, J.; Aspinwall, M.J.; Bellasio, C.; Bernacchi, C.; et al. A Reporting Format for Leaf-Level Gas Exchange Data and Metadata. *Ecol. Inform.* **2021**, *61*, 101232. [CrossRef]
32. Reich, P.B.; Walters, M.B.; Ellsworth, D.S. From Tropics to Tundra: Global Convergence in Plant Functioning. *Proc. Natl. Acad. Sci. USA* **1997**, *94*, 13730. [CrossRef]
33. Wright, I.J.; Reich, P.B.; Westoby, M.; Ackerly, D.D.; Baruch, Z.; Bongers, F.; Cavender-Bares, J.; Chapin, T.; Cornelissen, J.H.C.; Diemer, M.; et al. The Worldwide Leaf Economics Spectrum. *Nature* **2004**, *428*, 821–827. [CrossRef] [PubMed]
34. Ali, A.A.; Xu, C.; Rogers, A.; McDowell, N.G.; Medlyn, B.E.; Fisher, R.A.; Wullschleger, S.D.; Reich, P.B.; Vrugt, J.A.; Bauerle, W.L.; et al. Global-Scale Environmental Control of Plant Photosynthetic Capacity. *Ecol. Appl.* **2015**, *25*, 2349–2365. [CrossRef] [PubMed]
35. Gouyon, A.; de Foresta, H.; Levang, P. Does 'Jungle Rubber' Deserve Its Name? An Analysis of Rubber Agroforestry Systems in Southeast Sumatra. *Agrofor. Syst.* **1993**, *22*, 181–206. [CrossRef]
36. Wu, J.; Liu, W.; Chen, C. Below-Ground Interspecific Competition for Water in a Rubber Agroforestry System May Enhance Water Utilization in Plants. *Sci. Rep.* **2016**, *6*, 19502. [CrossRef]
37. Baltzer, J.L.; Thomas, S.C.; Nilus, R.; Burslem, D.F.R.P. Edaphic Specialization in Tropical Trees: Physiological Correlates and Responses to Reciprocal Transplantation. *Ecology* **2005**, *86*, 3063–3077. [CrossRef]
38. Kurokawa, H.; Yoshida, T.; Nakamura, T.; Lai, J.; Nakashizuka, T. The Age of Tropical Rain-Forest Canopy Species, Borneo Ironwood (Eusideroxylon Zwageri), Determined by 14C Dating. *J. Trop. Ecol.* **2003**, *19*, 1–7. [CrossRef]
39. Irawan, B. Growth Performance of One Year Old Seedlings of Ironwood (Eusideroxylon Zwageri Teijsm. & Binn.) Varieties. *J. Manaj. Hutan Trop.* **2012**, *18*, 184–190.
40. de Pury, D.G.G.; Farquhar, G.D. Simple Scaling of Photosynthesis from Leaves to Canopies without the Errors of Big-Leaf Models. *Plant Cell Environ.* **1997**, *20*, 537–557. [CrossRef]
41. Leuning, R.; Kelliher, F.M.; de Pury, D.G.G.; Schulze, E.-D. Leaf Nitrogen, Photosynthesis, Conductance and Transpiration: Scaling from Leaves to Canopies. *Plant Cell Environ.* **1995**, *18*, 1183–1200. [CrossRef]
42. Drescher, J.; Rembold, K.; Allen, K.; Beckschäfer, P.; Buchori, D.; Clough, Y.; Faust, H.; Fauzi, A.M.; Gunawan, D.; Hertel, D.; et al. Ecological and Socio-Economic Functions across Tropical Land Use Systems after Rainforest Conversion. *Philos. Trans. R. Soc. Lond. B Biol. Sci.* **2016**, *371*. [CrossRef] [PubMed]
43. Kotowska, M.M.; Leuschner, C.; Triadiati, T.; Hertel, D. Conversion of Tropical Lowland Forest Reduces Nutrient Return through Litterfall, and Alters Nutrient Use Efficiency and Seasonality of Net Primary Production. *Oecologia* **2016**, *180*, 601–618. [CrossRef] [PubMed]
44. Meijide, A.; Badu, C.S.; Moyano, F.; Tiralla, N.; Gunawan, D.; Knohl, A. Impact of Forest Conversion to Oil Palm and Rubber Plantations on Microclimate and the Role of the 2015 ENSO Event. *Agric. For. Meteorol.* **2018**, *252*, 208–219. [CrossRef]
45. Allen, K.; Corre, M.D.; Kurniawan, S.; Utami, S.R.; Veldkamp, E. Spatial Variability Surpasses Land-Use Change Effects on Soil Biochemical Properties of Converted Lowland Landscapes in Sumatra, Indonesia. *Geoderma* **2016**, *284*, 42–50. [CrossRef]
46. Hassler, E.; Corre, M.D.; Kurniawan, S.; Veldkamp, E. Soil Nitrogen Oxide Fluxes from Lowland Forests Converted to Smallholder Rubber and Oil Palm Plantations in Sumatra, Indonesia. *Biogeosciences* **2017**, *14*, 2781–2798. [CrossRef]
47. Chandrashekar, T.R.; Nazeer, M.A.; Marattukalam, J.G.; Prakash, G.P.; Annamalainathan, K.; Thomas, J. An Analysis of Growth and Drought Tolerance in Rubber during the Immature Phase in a Dry Subhumid Climate. *Exp. Agric.* **1998**, *34*, 287–300. [CrossRef]
48. Saputra, J.; Stevanus, C.T.; Cahyo, A.N. The Effect of El-Nino 2015 on the Rubber Plant (Hevea Brasiliensis) Growth in the Experimental Field Sembawa Research Centre. *Widyariset* **2016**, *2*, 37–46. [CrossRef]
49. Purwaningrum, Y.; Asbur, Y. Junaidi Latex Quality and Yield Parameters of Hevea Brasiliensis (Willd. Ex A. Juss.) Mull.Arg.Clone PB260 for Different Tapping and Stimulant Application Frequencies. *Chil. J. Agric. Res.* **2019**, *79*, 347–355. [CrossRef]
50. Cahyo, A.N.; Stevanus, C.T.; Aji, M. Production of PB260 Rubber Clone in Relation with Field Water Balance. In Proceedings of the International Rubber Conference, Jakarta, Indonesia, 15–18 November 2017; pp. 763–773.

51. Albert, L.P.; Wu, J.; Prohaska, N.; de Camargo, P.B.; Huxman, T.E.; Tribuzy, E.S.; Ivanov, V.Y.; Oliveira, R.S.; Garcia, S.; Smith, M.N.; et al. Age-Dependent Leaf Physiology and Consequences for Crown-Scale Carbon Uptake during the Dry Season in an Amazon Evergreen Forest. *New Phytol.* **2018**, *219*, 870–884. [CrossRef]
52. Koch, G.W.; Amthor, J.S.; Goulden, M.L. Diurnal Patterns of Leaf Photosynthesis, Conductance and Water Potential at the Top of a Lowland Rain Forest Canopy in Cameroon: Measurements from the Radeau Des Cimes. *Tree Physiol.* **1994**, *14*, 347–360. [CrossRef]
53. von Caemmerer, S.; Farquhar, G.D. Some Relationships between the Biochemistry of Photosynthesis and the Gas Exchange of Leaves. *Planta* **1981**, *153*, 376–387. [CrossRef]
54. Duursma, R.A. Plantecophys—An R Package for Analysing and Modelling Leaf Gas Exchange Data. *PLoS ONE* **2015**, *10*, e0143346. [CrossRef] [PubMed]
55. Medlyn, B.E.; Dreyer, E.; Ellsworth, D.; Forstreuter, M.; Harley, P.C.; Kirschbaum, M.U.F.; Le Roux, X.; Montpied, P.; Strassemeyer, J.; Walcroft, A.; et al. Temperature Response of Parameters of a Biochemically Based Model of Photosynthesis. II. A Review of Experimental Data. *Plant Cell Environ.* **2002**, *25*, 1167–1179. [CrossRef]
56. Farquhar, G.; Wong, S. An Empirical Model of Stomatal Conductance. *Funct. Plant Biol.* **1984**, *11*, 191–210. [CrossRef]
57. Norby, R.J.; Gu, L.; Haworth, I.C.; Jensen, A.M.; Turner, B.L.; Walker, A.P.; Warren, J.M.; Weston, D.J.; Xu, C.; Winter, K. Informing Models through Empirical Relationships between Foliar Phosphorus, Nitrogen and Photosynthesis across Diverse Woody Species in Tropical Forests of Panama. *New Phytol.* **2017**, *215*, 1425–1437. [CrossRef]
58. Niinemets, Ü.; Keenan, T.F.; Hallik, L. A Worldwide Analysis of Within-Canopy Variations in Leaf Structural, Chemical and Physiological Traits across Plant Functional Types. *New Phytol.* **2015**, *205*, 973–993. [CrossRef] [PubMed]
59. Lloyd, J.; Patiño, S.; Paiva, R.Q.; Nardoto, G.B.; Quesada, C.A.; Santos, A.J.B.; Baker, T.R.; Brand, W.A.; Hilke, I.; Gielmann, H.; et al. Optimisation of Photosynthetic Carbon Gain and Within-Canopy Gradients of Associated Foliar Traits for Amazon Forest Trees. *Biogeosciences* **2010**, *7*, 1833–1859. [CrossRef]
60. Lowman, M.D. Leaf Growth Dynamics and Herbivory in Five Species of Australian Rain- Forest Canopy Trees. *J. Ecol.* **1992**, *80*, 433–447. [CrossRef]
61. Kitajima, K.; Mulkey, S.S.; Wright, S.J. Variation in Crown Light Utilization Characteristics among Tropical Canopy Trees. *Ann. Bot.* **2005**, *95*, 535–547. [CrossRef]
62. Posada, J.M.; Lechowicz, M.J.; Kitajima, K. Optimal Photosynthetic Use of Light by Tropical Tree Crowns Achieved by Adjustment of Individual Leaf Angles and Nitrogen Content. *Ann. Bot.* **2009**, *103*, 795–805. [CrossRef]
63. Rijkers, T.; Pons, T.L.; Bongers, F. The Effect of Tree Height and Light Availability on Photosynthetic Leaf Traits of Four Neotropical Species Differing in Shade Tolerance. *Funct. Ecol.* **2000**, *14*, 77–86. [CrossRef]
64. Thomas, S.C.; Bazzaz, F.A. Asymptotic Height as a Predictor of Photosynthetic Characteristics in Malaysian Rain Forest Trees. *Ecology* **1999**, *80*, 1607–1622. [CrossRef]
65. Domingues, T.F.; Berry, J.A.; Martinelli, L.A.; Ometto, J.P.H.B.; Ehleringer, J.R. Parameterization of Canopy Structure and Leaf-Level Gas Exchange for an Eastern Amazonian Tropical Rain Forest (Tapajós National Forest, Pará, Brazil). *Earth Interact.* **2005**, *9*, 1–23. [CrossRef]
66. Buckley, T.; Miller, J.; Farquhar, G. The Mathematics of Linked Optimisation for Water and Nitrogen Use in a Canopy. *Silva Fenn.* **2002**, *36*, 639–669. [CrossRef]
67. Meir, P.; Kruijt, B.; Broadmeadow, M.; Barbosa, E.; Kull, O.; Carswell, F.; Nobre, A.; Jarvis, P.G. Acclimation of Photosynthetic Capacity to Irradiance in Tree Canopies in Relation to Leaf Nitrogen Concentration and Leaf Mass per Unit Area. *Plant Cell Environ.* **2002**, *25*, 343–357. [CrossRef]
68. Wright, I.J.; Leishman, M.R.; Read, C.; Westoby, M. Gradients of Light Availability and Leaf Traits with Leaf Age and Canopy Position in 28 Australian Shrubs and Trees. *Funct. Plant Biol.* **2006**, *33*, 407–419. [CrossRef]
69. Kosugi, Y.; Takanashi, S.; Yokoyama, N.; Philip, E.; Kamakura, M. Vertical Variation in Leaf Gas Exchange Parameters for a Southeast Asian Tropical Rainforest in Peninsular Malaysia. *J. Plant Res.* **2012**, *125*, 735–748. [CrossRef] [PubMed]
70. Niinemets, Ü.; Tenhunen, J.D. A Model Separating Leaf Structural and Physiological Effects on Carbon Gain along Light Gradients for the Shade-Tolerant Species Acer Saccharum. *Plant Cell Environ.* **1997**, *20*, 845–866. [CrossRef]
71. Niinemets, Ü.; Kull, O.; Tenhunen, J.D. An Analysis of Light Effects on Foliar Morphology, Physiology, and Light Interception in Temperate Deciduous Woody Species of Contrasting Shade Tolerance. *Tree Physiol.* **1998**, *18*, 681–696. [CrossRef]
72. Lawrence, D.M.; Fisher, R.A.; Koven, C.D.; Oleson, K.W.; Swenson, S.C.; Bonan, G.; Collier, N.; Ghimire, B.; van Kampenhout, L.; Kennedy, D.; et al. The Community Land Model Version 5: Description of New Features, Benchmarking, and Impact of Forcing Uncertainty. *J. Adv. Modeling Earth Syst.* **2019**, *11*, 4245–4287. [CrossRef]
73. Fisher, R.A.; Wieder, W.R.; Sanderson, B.M.; Koven, C.D.; Oleson, K.W.; Xu, C.; Fisher, J.B.; Shi, M.; Walker, A.P.; Lawrence, D.M. Parametric Controls on Vegetation Responses to Biogeochemical Forcing in the CLM5. *J. Adv. Modeling Earth Syst.* **2019**, *11*, 2879–2895. [CrossRef]
74. Kumagai, T.; Mudd, R.G.; Miyazawa, Y.; Liu, W.; Giambelluca, T.W.; Kobayashi, N.; Lim, T.K.; Jomura, M.; Matsumoto, K.; Huang, M.; et al. Simulation of Canopy CO_2/H_2O Fluxes for a Rubber (Hevea Brasiliensis) Plantation in Central Cambodia: The Effect of the Regular Spacing of Planted Trees. *Ecol. Model.* **2013**, *265*, 124–135. [CrossRef]
75. Olchev, A.; Radler, K.; Sogachev, A.; Panferov, O.; Gravenhorst, G. Application of a Three-Dimensional Model for Assessing Effects of Small Clear-Cuttings on Radiation and Soil Temperature. *Ecol. Model.* **2009**, *220*, 3046–3056. [CrossRef]

76. Widlowski, J.-L.; Pinty, B.; Clerici, M.; Dai, Y.; De Kauwe, M.; de Ridder, K.; Kallel, A.; Kobayashi, H.; Lavergne, T.; Ni-Meister, W.; et al. RAMI4PILPS: An Intercomparison of Formulations for the Partitioning of Solar Radiation in Land Surface Models. *J. Geophys. Res. Biogeosci.* **2011**, *116*. [CrossRef]
77. Rival, A. *Achieving Sustainable Cultivation of Oil Palm Volume 1: Introduction, Breeding and Cultivation Techniques*, 1st ed.; Burleigh Dodds Science Publishing: Hong Kong, China, 2018.
78. Kenzo, T.; Ichie, T.; Watanabe, Y.; Yoneda, R.; Ninomiya, I.; Koike, T. Changes in Photosynthesis and Leaf Characteristics with Tree Height in Five Dipterocarp Species in a Tropical Rain Forest. *Tree Physiol.* **2006**, *26*, 865–873. [CrossRef] [PubMed]
79. Meir, P.; Levy, P.E.; Grace, J.; Jarvis, P.G. Photosynthetic Parameters from Two Contrasting Woody Vegetation Types in West Africa. *Plant Ecol.* **2007**, *192*, 277–287. [CrossRef]
80. Leuning, R.; Dunin, F.X.; Wang, Y.-P. A Two-Leaf Model for Canopy Conductance, Photosynthesis and Partitioning of Available Energy. II. Comparison with Measurements. *Agric. For. Meteorol.* **1998**, *91*, 113–125. [CrossRef]
81. Kositsup, B.; Kasemsap, P.; Thanisawanyangkura, S.; Chairungsee, N.; Satakhun, D.; Teerawatanasuk, K.; Ameglio, T.; Thaler, P. Effect of Leaf Age and Position on Light-Saturated CO_2 Assimilation Rate, Photosynthetic Capacity, and Stomatal Conductance in Rubber Trees. *Photosynthetica* **2010**, *48*, 67–78. [CrossRef]
82. Corley, R.H.V. Photosynthesis and Age of Oil Palm Leaves. *Photosynthetica* **1983**, *17*, 97–100.
83. Apichatmeta, K.; Sudsiri, C.J.; Ritchie, R.J. Photosynthesis of Oil Palm (Elaeis Guineensis). *Sci. Hortic.* **2017**, *214*, 34–40. [CrossRef]
84. Meijide, A.; Röll, A.; Fan, Y.; Herbst, M.; Niu, F.; Tiedemann, F.; June, T.; Rauf, A.; Hölscher, D.; Knohl, A. Controls of Water and Energy Fluxes in Oil Palm Plantations: Environmental Variables and Oil Palm Age. *Agric. For. Meteorol.* **2017**, *239*, 71–85. [CrossRef]
85. Stiegler, C.; Meijide, A.; Fan, Y.; Ashween Ali, A.; June, T.; Knohl, A. El Niño–Southern Oscillation (ENSO) Event Reduces CO_2 Uptake of an Indonesian Oil Palm Plantation. *Biogeosciences* **2019**, *16*, 2873–2890. [CrossRef]
86. Fan, Y.; Roupsard, O.; Bernoux, M.; Le Maire, G.; Panferov, O.; Kotowska, M.M.; Knohl, A. A Sub-Canopy Structure for Simulating Oil Palm in the Community Land Model (CLM-Palm): Phenology, Allocation and Yield. *Geosci. Model Dev.* **2015**, *8*, 3785–3800. [CrossRef]
87. Ibrom, A.; Oltchev, A.; June, T.; Kreilein, H.; Rakkibu, G.; Ross, T.; Panferov, O.; Gravenhorst, G. Variation in Photosynthetic Light-Use Efficiency in a Mountainous Tropical Rain Forest in Indonesia. *Tree Physiol.* **2008**, *28*, 499–508. [CrossRef]
88. Pearse, G.D.; Watt, M.S.; Morgenroth, J. Comparison of Optical LAI Measurements under Diffuse and Clear Skies after Correcting for Scattered Radiation. *Agric. For. Meteorol.* **2016**, *221*, 61–70. [CrossRef]